Inventory of complex, cascading and compound disaster events in Europe

Deliverable D1.3

Release Status: FINAL
Dissemination Level: Public
Authors: Shadi Shirazian, Maria Luisa Colmenares, Judith Claassen, Elco Koks
Date: 31/10/2024
File name and Version: D1.3 MIRACA.pdf
Project ID Number: 101093854
Call: HORIZON-MISS-2021-CLIMA-02-03
DG/Agency: CINEA

This project has received funding from the European Union's horizon Europe research and innovation program under grant agreement No. 101093854

Document History

Revision History

Version No.	Revision Date	Filename / Location Stored	Summary of Changes
V01	01/04/2024	D1.3.docx	First Version
Final	11/07/2024	D1.3 MIRACA.pdf	Final Version
Revised	31/10/2024	D1.3 MIRACA.pdf	Revised Final Version

Authorization
This document requires the following approvals:

Name	Authorization	Signature	Date of Issue
Stavroula Fotopoulou	WP Leader	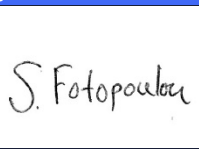	31/10/2024
Elco Koks	Project Coordinator	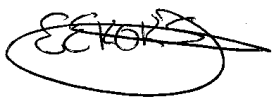	31/10/2024

Distribution
This project is distributed to:

Name	Title	Version issued	Date of Issue
Elco Koks	Project Coordinator	Final	31/10/2024

This project has received funding from the European Union's horizon Europe research and innovation program under grant agreement No. 101093854

Table of Contents

This project has received funding from the European Union's horizon Europe research and innovation program under grant agreement No. 101093854

1. Introduction

Multi-hazard events are groups of hazards that can occur simultaneously or with a temporal delay, either independently or as secondary hazards triggered by an initial hazard. This can cause cascading effects and significantly impact an area, often much more than single hazards (De Ruiter et al. 2020). Ignoring the possibility of multi-hazard occurrences can lead to underestimating the risk, jeopardizing efforts to enhance resilience. Aligned with the scope of the MIRACA project, which aims to improve the adaptability of critical infrastructures in Europe to natural hazards, this deliverable, related to Task 1.3, focuses on creating an event set for each single hazard, including climatological (drought, heatwave, windstorm, wildfire), hydrological (flood), and geological (earthquake and landslides), and then a multi-hazard event dataset of natural hazards.

Box 1: Definition of different multi-hazard as used within the MIRACA project

We use the United Nations Disaster Risk Reduction (UNDRR) definition of multi-hazard below:

- *Multi-Hazard*: (1) the selection of multiple major hazards that a region faces, and (2) the specific contexts where hazardous events may occur simultaneously, cascading, or cumulatively over time.
- *Compound relationships*: Two or more hazards coinciding in space and/or time (e.g., a coastal flood and a river flood occurring in the same region).
- *Cascading disasters*: a primary hazard triggering a secondary hazard.
- *Consecutive disasters*: two or more disasters that occur in succession, and whose direct impacts overlap spatially before recovery from a previous event is considered to be completed.

Event sets of hazards are essential data for loss modeling of infrastructures. To calculate loss metrics that reflect the loss of network functionality, such as connectivity loss and time delays, it is necessary to estimate the damage to network components from each particular event. Moreover, to create a dataset of multi-hazard events, scenarios of single hazards that include the footprint of events and the times of their start and end are needed to identify events that spatially and temporally overlap. Moreover, these event sets provide an important input for the five Use Cases, as outlined in Figure 1.

This project has received funding from the European Union's horizon Europe research and innovation program under grant agreement No. 101093854

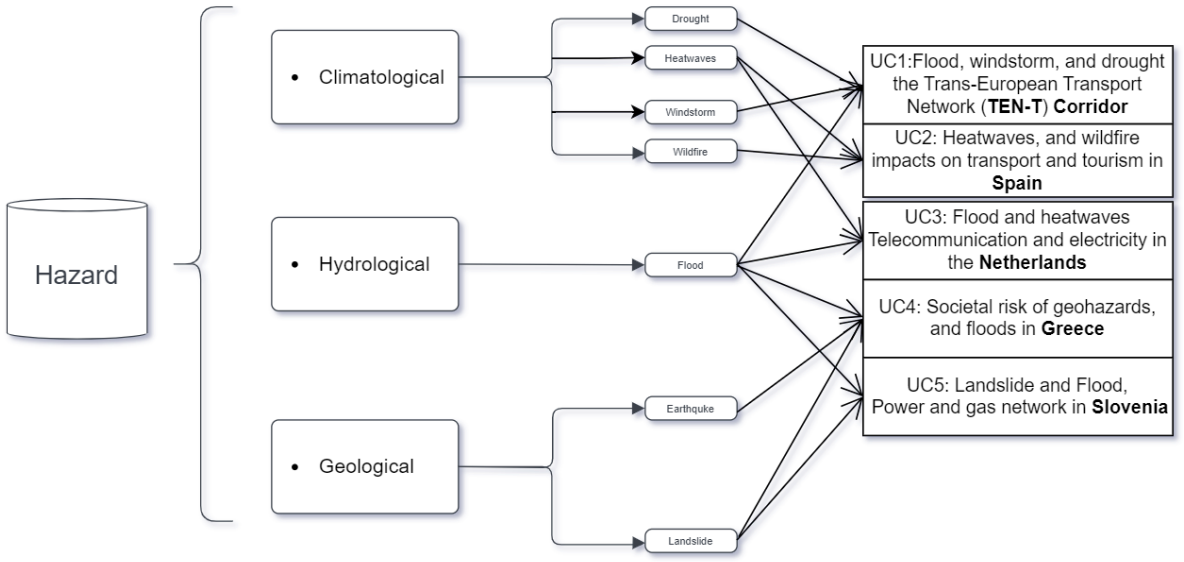

Fig.1. *Connection of the various geological, climatological and hydrological hazards to the five use cases.*

Deliverable 1.3 (D1.3) builds upon the database constructed in Deliverable 1.2 (D1.2), where we have provided a comprehensive catalog of reliable hazard resources specifically for Europe, making it an invaluable starting point for gathering hazard data. For certain hazards, such as windstorms, drought, landslides, and heatwaves, we utilized the same references listed in D1.2. However, the hazard data in D1.2—for example, on floods, earthquakes, and wildfires—primarily focuses on hazard maps or catalogues, rather than data on individual events. Moreover, the presented flood event set in D1.3 has only been published after the submission of D1.2. D1.3 requires the collection of historical event data, including each event's footprint, intensity measures, timing, and duration. Therefore, we identified additional references that specifically provide these details for single event sets. D1.2 has been updated accordingly.

In this task, single hazard data is first collected for each hazard. It is ensured that each event includes a polygon, start and end times, and an intensity measure. For generating the multi-hazard event set, the MYRIAD-Hazard Event Sets Algorithm (MYRIAD-HESA), developed by Claassen et al. (2023), is applied. This algorithm compares the events in single hazards and creates groups of events that spatially and temporally overlap. It also provides the possibility of defining a time lag for the events that shape a group of events within the multi-hazard event set. The algorithm requires creating a list of

This project has received funding from the European Union's horizon Europe research and innovation program under grant agreement No. 101093854

information for each hazard, including the start time, end time, and polygon of the event footprint.

The first section of this deliverable is a review of the single events for each hazard that were collected or, in some cases, created. The second section explains the applied algorithm in developing the multi-hazard event set and the resulting multi-hazard event sets. It should be mentioned that two types of multi-hazard event sets were developed: one without considering any temporal delay between events and the other with a 4-day time lag between events. The results will be compared in the discussion section.

2. Methods

For each of the seven hazards in this task, (Drought, Heatwave, Windstorm, Wildfire, Flood, Earthqauke, and Landslide), a comprehensive search for data was conducted, and single event data sets were collected. These events are derived from historical, modeled, or reanalysis data. In cases where single events were available, they were utilized directly; otherwise, events were generated based on assumptions such as thresholds for the damaging intensity of the hazard, buffer zones, and clustering methodologies (see Section 3).

To generate multi-hazard event sets, here we use the algorithm developed by Claassen et al. (2023). This algorithm (MYRIAD-HESA) uses single hazard event data to determine the location and timing of each hazard. Each event is represented by a polygon indicating its spatial extent and includes start and end dates, as well as intensity, although intensity is only used in creating the final multi-hazard event set. Hazards form a pair if their event polygons and timeframes overlap.

This project has received funding from the European Union's horizon Europe research and innovation program under grant agreement No. 101093854

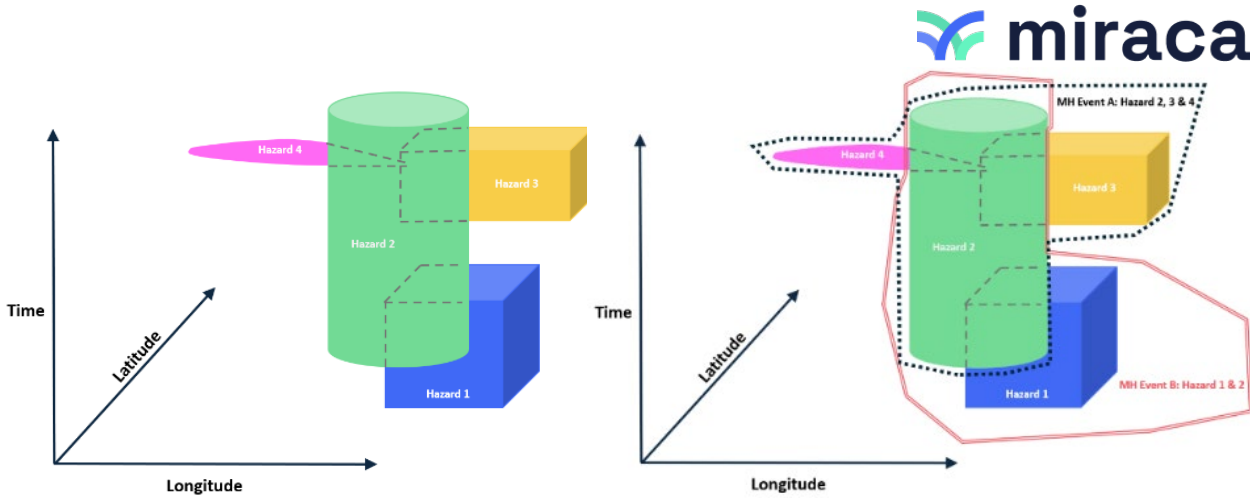

Fig. 2: 3D Illustration of the Algorithm for Generating Multi-Hazard Event Sets. Part (a) shows the coordinate axes and the time axis to demonstrate the two criteria of time and location in grouping. Hazards 1, 2, 3, and 4 occur sequentially. The grey dashed lines are used to depict the boundaries of hazard that lie inside the boundary of the other hazard. Part (b) shows the two multi-hazard (MH) events resulting from grouping the single hazard events that temporally and spatially overlapped.

Once hazard pairs are identified, they are grouped into multi-hazard events if all individual hazards in the pairs overlap. Figure 2 is a 3D illustration of the applied overlapping method. For example, if pairs (Hazard 2, Hazard 3) and (Hazard 2, Hazard 4) exist, they form a group if (Hazard 2, Hazard 4) also exists. The algorithm can introduce a time-lag, allowing a second event to occur within a specified number of days after the first, provided they overlap spatially. This approach captures multi-hazard events that do not overlap directly in time.

3. Single hazard datasets

In collecting event scenarios, each event should include the polygon of the area that was exposed to the event, the start time and end time of the event, as well as an intensity measure map that reflects the severity of the hazard per coordinate to be used in further loss modeling of the infrastructures (Claassen et al., 2023). However, this data is not readily available for all types of hazards. Therefore, in cases where we face a lack of data, some engineering judgments and assumptions are implemented. The sources of data for this task are either recordings from historical events or from empirical models or reanalysis.

This project has received funding from the European Union's horizon Europe research and innovation program under grant agreement No. 101093854

3.1 Drought

According to European Drought Observatory (EDO), several parts of Europe are at the risk of drought like Spain, Italy, Romania, Poland, Baltic regions, most of Greece, northern Balkans, and the Mediterranean islands (Joint Research Centre, 2024). The increasing risk of drought in Europe can be due to global warming and low precipitation rates (Suarez-Gutierrez et al 2023) due to climate change. As noted in the Low Flow Index factsheet by the Joint Research Centre (JRC), droughts can be categorized into three types: agricultural, meteorological, and hydrological. Agricultural drought is related to low soil moisture, which reduces crop production. Meteorological drought refers to periods of below-average rainfall in a region, while Hydrological drought pertain reduced water availability in rivers and reservoirs (European Commission, Joint Research Centre, 2018). Different indicators might be used for different drought types for instance indicators that refer to temperature and precipitation are used for meteorological droughts or indicators that are related to water level, streamflow can be used for hydrological droughts (Bachmair et al. 2016).

Here, concerning hydrological droughts and the exposure of inland waterways, data for the low flow index (LFI) from the JRC for the years 1995 to 2022, version 2.1.0, are collected. To define drought events, a threshold of 0.5 for LFI, indicating high drought risk, was considered. Additionally, a buffer area of 10 km around the drought area is created to increase the chance of overlapping with other events and facilitate the generation of multi-hazard event sets, based on the assumption that areas in direct proximity to the river, particularly those with economic activities, are potentially impacted by low river flows.

This project has received funding from the European Union's horizon Europe research and innovation program under grant agreement No. 101093854

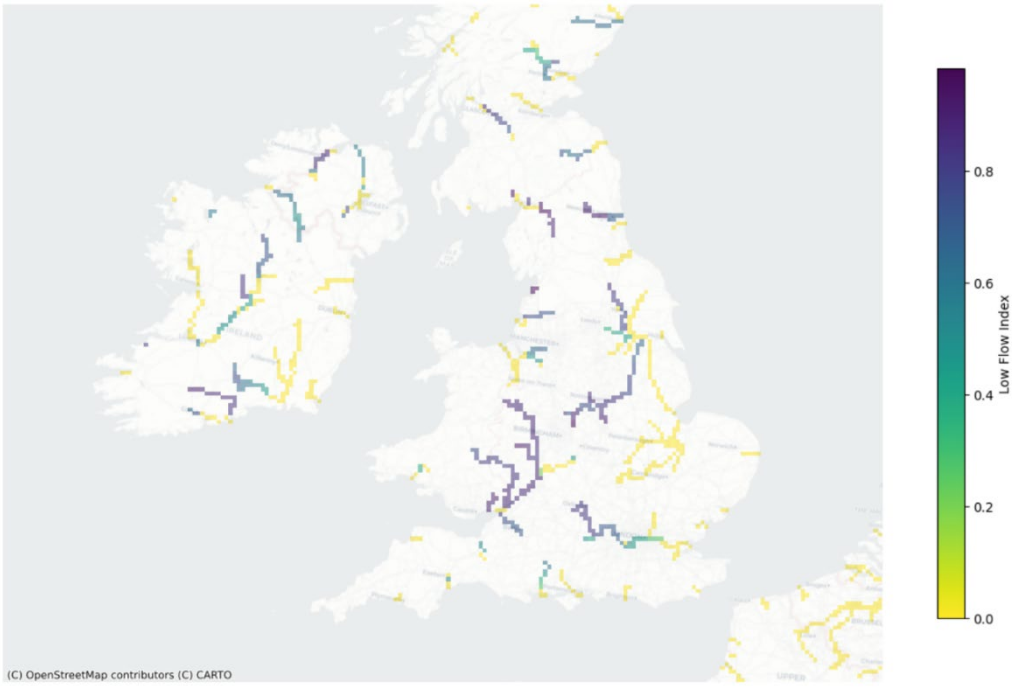

Fig 3: *Sample of spatial extent of Low flow indices for the United Kingdom*

Drought	Source	• Joint Research Centre (JRC)			
	Data	Drought indicators	EDO Low Flow Index (LFI): .1995-2022	Main Parameter	• LFI
				Version	2.1.0
				File format	NetCDF
				Horizontal Resolution	5 kilometer

3.2 Heatwave

The ERA5 reanalysis data on temperature, for the years 1987 to 2023, has been collected from the Copernicus Climate Data Store (Hersbach et al. 2023). The data represents the hourly temperature at 2 meters above the surface of the land or sea, measured in Kelvin. To create the heatwave events, the hourly temperature per grid was first converted to the daily mean per grid. Then, the rolling 95th percentile for a time window of 10 years for each date and each grid was calculated and compared with the daily mean temperature for each date and each grid. If the daily mean is greater than its rolling 95th percentile, that day is considered a hot day. A heatwave event is defined in one spatial

This project has received funding from the European Union's horizon Europe research and innovation program under grant agreement No. 101093854

grid if there is a hot day for at least three consecutive days. Additionally, a lower temperature limit of 30°C, or 303.15 K, is set to exclude relatively moderate events. Here we deviate from the standard definition of a heatwave, which generally only assumes the exceedance of the 95th percentile for at least three consecutive days. This could also happen during winter time. For infrastructure systems, we are most interested in temperatures that may go beyond the design standards of the infrastructure assets (St Cloud 2022). A clustering algorithm is applied to group those events that occur in adjacent grids at the same time. When the group of events is created, the maximum temperature within the events of the same group is considered the temperature of the group.

Fig 4: *The spatial extent of a heatwave event*

Heatwaves	Source	• ERA5, Copernicus Climate Data Store			
	Data	Temperature	T2m (Kelvin): •1987-2023	Main Parameter	• T2m (Kelvin)
				Version	
				File format	NetCDF
				Horizontal Resolution	~0.25° *0.25°

This project has received funding from the European Union's horizon Europe research and innovation program under grant agreement No. 101093854

3.3 Windstorm

The winter windstorm footprints are collected from Copernicus Climate Data (Copernicus Climate Data Store, 2022) for the months from October to March and the years 1979 to 2021. This data is derived from ERA5 reanalysis, and the intensity measure for the wind speed is the maximum speed of a 2-second wind gust at 10m height within 72 hours, measured in meters per second (m/s). To identify windstorm events, a threshold of 35 m/s is used.

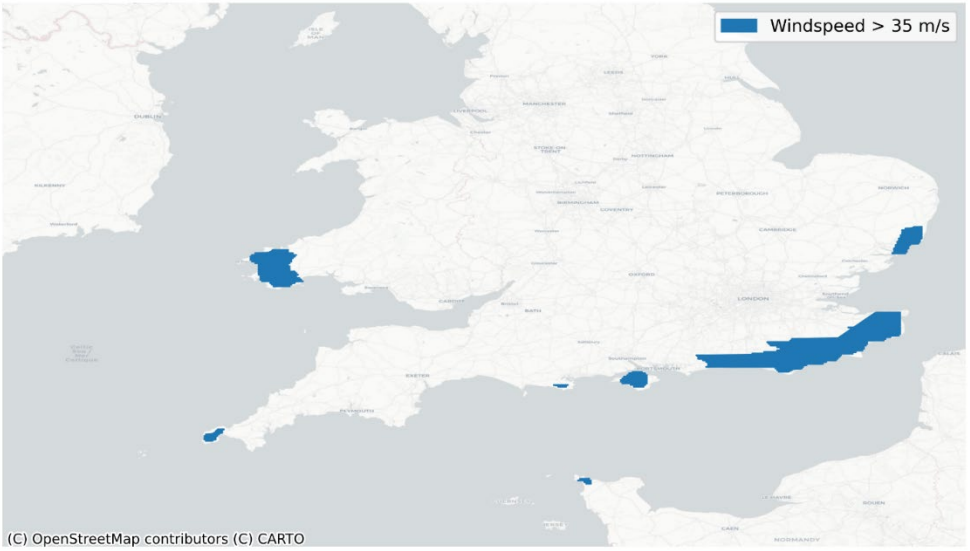

Fig 5: *Windstorm spatial extent from the data set*

Windstorm	Source	• Copernicus Climate Data Store			
	Data	Footprints	Reanalysis of historical events: •1979-2021, Oct-March	Main Parameter	• Maximum speed of 3- second wind gust at 10m height within 72 h, (m/s)
				Number of events	118
				File format	NetCDF
				Horizontal Resolution	1.0 km

This project has received funding from the European Union's horizon Europe research and innovation program under grant agreement No. 101093854

3.4 Wildfire

The footprint of about 70,000 wildfire events (San-Miguel-Ayanz et al., 2012) in Europe from 2000 to 2024 were collected from the European Forest Fire Information System (EFFIS) of the European Commission Joint Research Centre. This dataset includes the polygon of the event, the start and end time of the event, and the area that is burnt (in hectares). In this dataset, from 2000 to 2005, there is incomplete information regarding the duration of the events, with multiple events unusually dated January 1st of 2001. We attempted to reconstruct the correct duration with information from different resources, through the use of the Global Fire Atlas (GFA) dataset (Andela et al., 2019). To obtain the correct duration based on the location of fire, we compared the overlapping events. Events with a similar burnt area (geospatially) are regarded as the same event and therefore the duration could be updated, corresponding to the GFA (Andela et al., 2019); however, the dataset from the GFA starts in 2003, so only events from 2003-2005 could be updated. Therefore, due to the lack of data for years between 2000 and 2003, the start and end times of the wildfires are identical in the final event set.

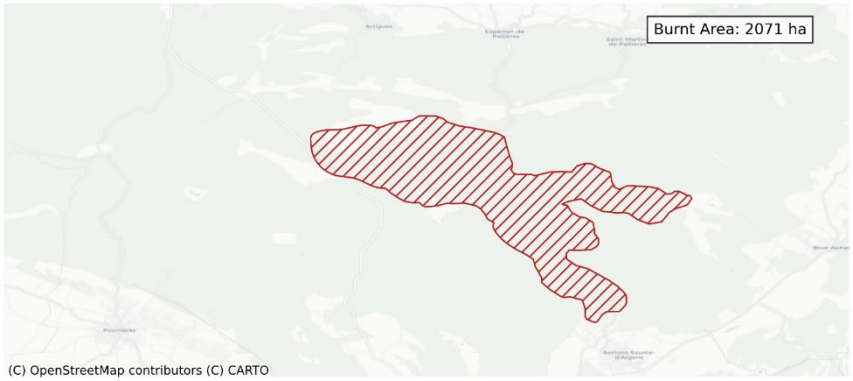

Fig 6: *The spatial extent of a wildfire sample from the data set and the area burnt*

Wildfire	Source	• European forest fire information system (EFFIS)		
	Data	Footprints: •2000-2024	Main Parameters	• Place • Start-end time • Area (hectare)
			Number of events	70479
			Version	1.1.0
			File format	Shapefile (vector)

This project has received funding from the European Union's horizon Europe research and innovation program under grant agreement No. 101093854

3.5 Flood

River flooding causes annual losses of around 7.6 billion euros in Europe and the UK, and this risk is expected to increase by the end of the century. Factors contributing to this risk include climate change and the growing exposure of populations and assets in flood-prone areas (Dottori et al., 2023). To increase the resilience of infrastructures against floods, it is crucial to estimate the potential losses from such events in the region in order to make informed decisions and apply risk mitigation measures.

Here, the modeled potential flood catalog from the study by Paprotny et al. (2024) is used. This catalog, including 15,000 modeled flood events for 42 countries in Europe spanning from 1950 to 2020, was generated through a chain of models integrating climate data, hydrodynamic models, and other factors, with the results validated against historical records. The database provides detailed information about each event, including the start and end dates, location, footprint, and water depth. While the maps of water depth for each flood event are not publicly available at the time of preparing this deliverable, we obtained this data for Task 1.3 directly from the authors of the research. A sample of the map of water depth for a flood event is shown in Fig. 7. The catalog and its associated data are accessible online through the publication by Paprotny et al. (2024).

This project has received funding from the European Union's horizon Europe research and innovation program under grant agreement No. 101093854

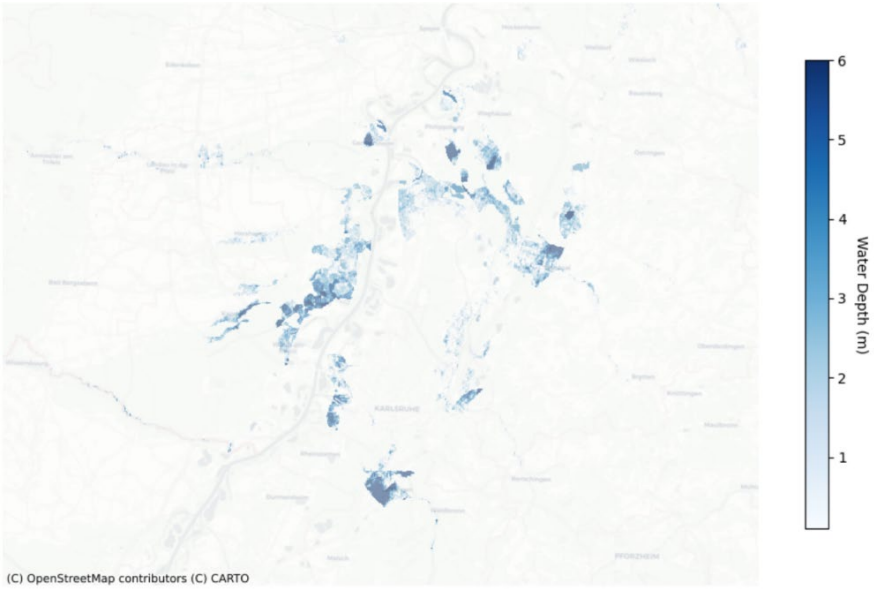

Fig 7: Footprint of a flood event including the water depth, from flood dataset (Paprotny et al 2024).

Flood	Sources	• Paprotny et al. 2024, HANZE catalogue of modelled and historical floods in Europe			
	DATA	Catalog and Footprints	Paprotny et al. 2024: 1950-2020	Parameters	• Place • Start-end time • Type of flood (River, flash, coastal) • Impacted regions • Inundated Area • Cause of the flood • Loss (fatality & economic in euros) • Also mentions hazard concurrency • Mean Water Depth (mm) • Return Period (years)
				Number of events	15000
				File format	Tiff and Shapefile (vector)

3.6 Earthquake

Earthquakes, a type of geohazard, are caused by the sudden release of energy due to tectonic movements or volcanic activities. The released energy can propagate in the form of waves towards the Earth's surface, causing ground shaking. Earthquakes can also trigger secondary hazards such as tsunamis, landslides, liquefaction, and surface

This project has received funding from the European Union's horizon Europe research and innovation program under grant agreement No. 101093854

ruptures. Infrastructures, which are spatially extended, can cross seismic-prone areas and thus be vulnerable to earthquakes.

In Europe, areas like Turkey, Italy, Greece, Romania, and Albania are high seismic areas due to their proximity to active tectonic boundaries. To create an earthquake event set, a catalog of earthquake events from 1900-2023 in Europe from USGS is collected, which includes information such as time, coordinates of the epicenter, depth, and magnitude of an event. Normally, a magnitude of 5.5 is the threshold for infrastructure concerns (Gua et al. 2017, and Li et al 2023), but for MIRACA, which also considers healthcare systems and schools as critical infrastructure, can be old masonry buildings that might not have been constructed based on seismic codes, a threshold of magnitude 4.5 is used for collecting earthquake data. Along with this catalog, packages of ShakeMap from USGS for each event in the catalog, including shapefiles of maps for several intensity measures (Peak Ground Acceleration (g), Peak Ground Velocity(cm/s), Spectral Acceleration(g) at 0.3s, 1s, and 3s natural periods, and Modified Mercalli Intensity), were collected.

As mentioned before, for generating multi-hazard events, we require a footprint for each event. For this reason, for Modified Mercalli Intensity maps, a threshold of MMI greater than 5, which is related to damaging earthquakes, is considered. In total, around 1000 earthquake events within Europe meet these conditions.

This project has received funding from the European Union's horizon Europe research and innovation program under grant agreement No. 101093854

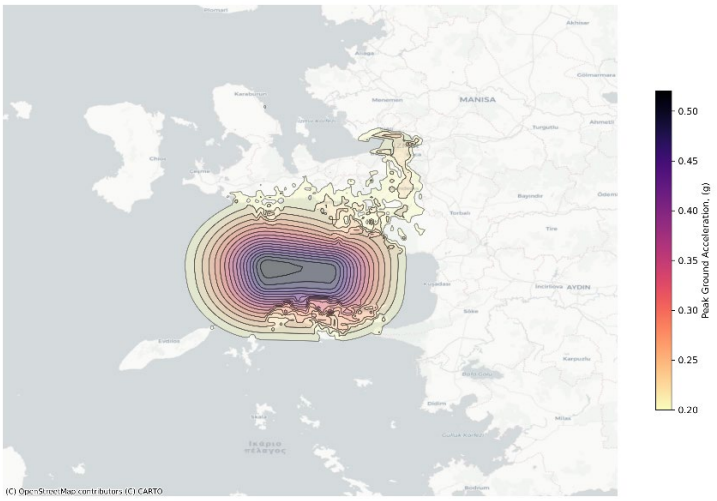

Fig 8: Map of PGA of an earthquake event in the dataset (USGS), here is plotted for PGA > 0.2 g.

Earthquake	Sources	• United States Geological Survey (USGS)			
	Data	Historical Catalog	USGS: For magnitudes > 4.5 •1905-2023	Parameters	Such as: • Place • Epicenter Coordinates • Depth • Time of the event • Magnitude
				Number of events	1100
				File format	csv
		Maps	USGS: Packages of ShakeMap •1905-2023	Parameters	• Peak Ground Acceleration, PGA (%g) • Spectral acceleration, SA 0.3s, 1s, 3s periods and for 5% damping,(%g) • Peak Ground Velocity PGV (cm/s) • Modified Mercalli Intensity
				Number of events	1100
				Selected version	Preferred
				File format	Shapefile (vector)

This project has received funding from the European Union's horizon Europe research and innovation program under grant agreement No. 101093854

3.7 Landslide

Landslides are a type of geohazard that mostly occur in sloped areas. Since infrastructures often extend across different topographies and soil types, they can be vulnerable to this hazard. The size of landslides ranges from very small to very large (McColl et al 2024), involving rocks, debris, and unstable soil sliding downward. Landslides can be triggered naturally by events such as earthquakes, volcanic activity, heavy rainfall, and erosion. They can also be triggered by human activities like improper mining.

Europe, with its diverse topography and soil types, has several areas prone to landslides, including Italy, Norway, Slovakia, Spain (Herrera et.al 2018), and Greece (Koukis et al., 2015). However, data about previous events in Europe, including their footprints, is not publicly available at the time of preparing this deliverable. Therefore, a catalogue of previous events developed by Kirschbaum et al. (2012, and 2015) and available at NASA is used here. This catalogue includes information such as the coordinates of a single point considered as the location of the landslide, the time, the trigger (e.g., rain-induced, earthquake-induced), and the size of the events. The size is defined by categorical variables: small, medium, large, very large, or unknown.

An approximate area classification following the study by McColl et al (2024), where the size of the events is classified by the area affected, is used here. Therefore, around the coordinates of the landslide location, an approximate radius from 0.0002° for small or unknown sizes of events to 0.50828° for very large ones is considered.

This project has received funding from the European Union's horizon Europe research and innovation program under grant agreement No. 101093854

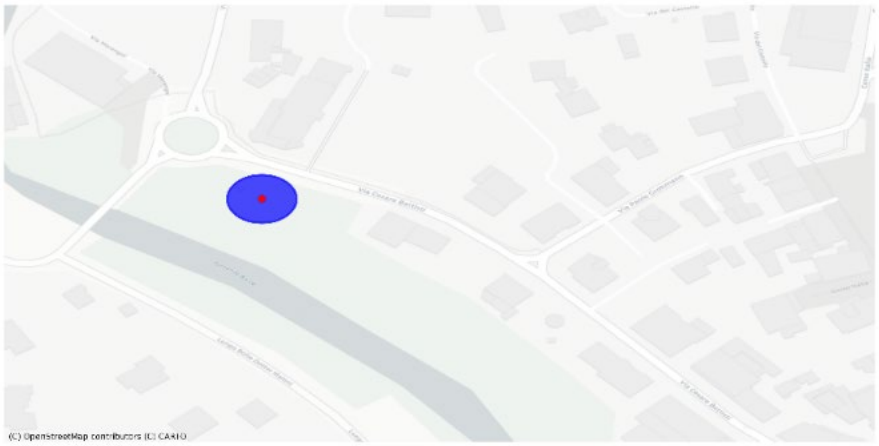

Fig 9: A sample of area that is considered for a landslide in the Landslide data set.

Landslides	Sources	• National Aeronautics and Space Administration (NASA)			
	Data	Historical Catalog	NASA: 1988-2017	Parameters	Such as: • Place • Coordinates • Size of the event (small, Medium, large, Unknown) • Time of the event • Landslide trigger (rainfall, earthquake etc.)
				Number of events*	539
				File format	csv

4. Multi-Hazard Event Set

Having an event set for each single hazard, in this section we group events from the seven types of hazards that temporally and spatially overlapped. These groups will form the Multi-Hazard (MH) event set. In creating the multi-hazard events, we first consider scenarios without any time lag between events, meaning the temporal overlap could only happen if the events occurred within the duration of another event. For the second set of MH events, we considered a time lag of four days, which is expected to result in more MH event cases.

It should be noted that in this task, we do not consider the dynamic nature of some hazards, such as wildfires, where the spatial extent of the event changes gradually over different time steps. Instead, we use the total extent and total duration as the spatial and temporal extent of the event.

This project has received funding from the European Union's horizon Europe research and innovation program under grant agreement No. 101093854

4.1. Multi-hazard event set without time lag

One of the multi-hazard (MH) event sets is created with no time lag. This means that events are only considered as a group if they spatially overlap and occur within the same time window. This assumption potentially overlooks the harmful cascading effects of events that occur immediately after each other, as it does not consider them as a multi-hazard event. However, this zero time lag approach, compared to the next section where time lag is considered, provides insight into the importance of considering a delay interval between events to include them in a multi-hazard event set.

The resulting MH dataset in this section contains 6,830 pairs of hazard events, 691 groups of 3 hazards, 49 groups of 4 hazards, and 1 group of 5 hazards, either as combinations of different or identical type of hazards. In Fig. 10 (a, b, c), the frequency of different combinations of hazards, including groups of 2, 3, and 4, is shown. Heatwave-wildfire and flood-drought pairs are the most frequent events, while drought-landslide and heatwave-landslide pairs are the least frequent in this MH dataset. Additionally, there are no concurrent landslide-earthquake pairs in this dataset. However, in our single hazard dataset, both the earthquake catalog and the landslide catalog individually include the Lefkada event from November 2015 in Greece, where an earthquake-induced landslide occurred, but there is a time delay between the occurrences of these two events in the single hazard catalogs.

When comparing all three plots in Figure 10, it is evident that the combination of windstorms and floods is one of the most commonly combinations. The number of groups of three hazards that include this combination is higher than the number of extreme wind-flood pairs. This is because the applied multi-hazard algorithm does not count events multiple times. Whether an event is part of a pair, a group of three, four, or more, it is only counted once within each grouping category.

These graphs collectively might highlight the prevalence and patterns of multi-hazard events, indicating that certain combinations of hazards are more likely to occur together even without any time lag. Of course, the nature of the data, more precisely the dominance or scarcity of certain events, plays a significant role in creating these combinations.

This project has received funding from the European Union's horizon Europe research and innovation program under grant agreement No. 101093854

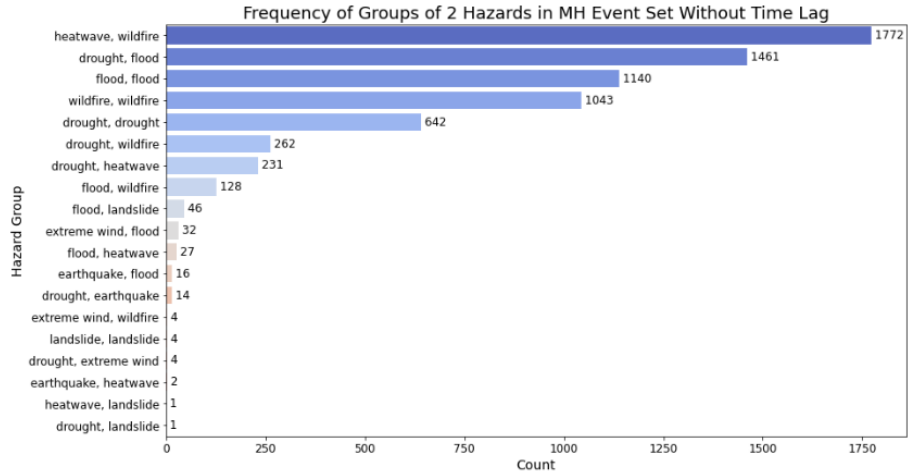

a) Groups of 2 hazards

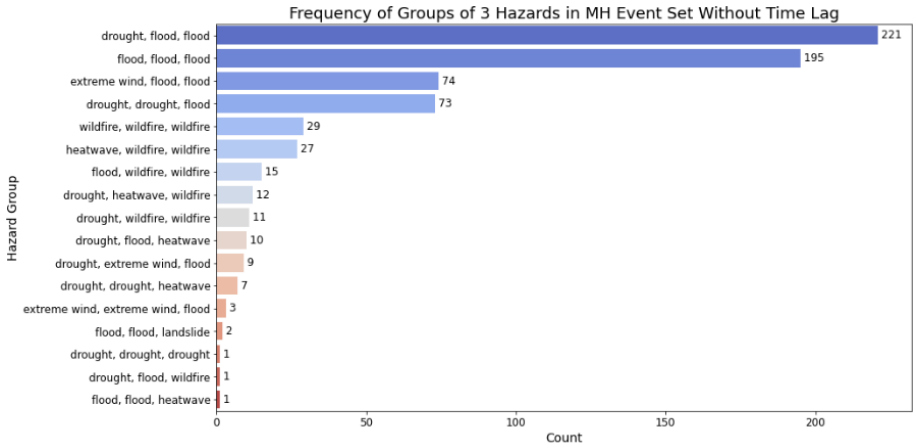

b) Groups of 3 hazards

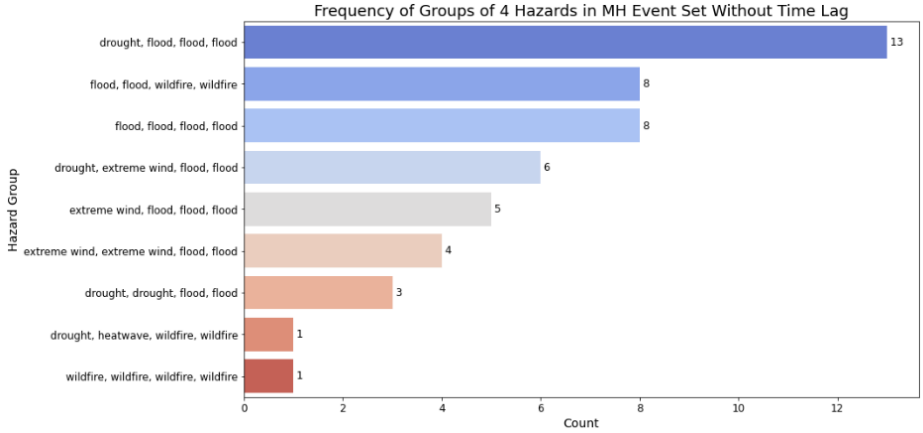

c) Groups of 4 hazards

Fig. 10: *a, b, & c the frequency of MH event sets without a time lag, groups of 2, 3, & 4 hazards respectively*

This project has received funding from the European Union's horizon Europe research and innovation program under grant agreement No. 101093854

4.2. Multi-hazard event set with a 4-day time lag

The second MH event set of this task is created with a 4-day time lag. Therefore, events that spatially overlap can also occur up to 4 days after another hazard. Initially, this 4-day assumption was intentionally chosen to include events known from history to be multi-hazard (such as the Lefkada event mentioned in the previous section). This approach also helps include other hazards, like earthquakes, which occur suddenly but might coincide with other hazards or even trigger them.

The resulted MH dataset in this section with a 4-day time lag contains 7,362 pair events, 904 groups of 3 hazards, 128 groups of 4 hazards, 8 groups of 5 hazards, and 1 group of 6 hazards. As expected, more events exist in each group compared to the MH event set without the time lag consideration. In Fig. 11 (a, b, c), the frequency of different combinations of hazards, including groups of 2, 3, and 4, is shown. According to part (a) of Figure 11, the highest number of MH events are pairs of heatwave-wildfire and flood-drought. Pairs of landslide-earthquake, landslide-heatwave, windstorm-landslide, and windstorm-windstorm are rare events in the dataset. This is still likely due to the lack of sufficient information about events, such as landslides which required assumptions about their spatial extent, as well as the limited number certain events in the dataset.

According to parts (b) and (c) of both Figures 10 and 11, in groups of 3 and 4 hazards, combinations of floods and droughts are more common. The large number of concurrent drought and flood events in both of our MH event sets may be due to the drought indicator we used, the LFI, which reflects the drought effect in river areas where floods can also occur.

This project has received funding from the European Union's horizon Europe research and innovation program under grant agreement No. 101093854

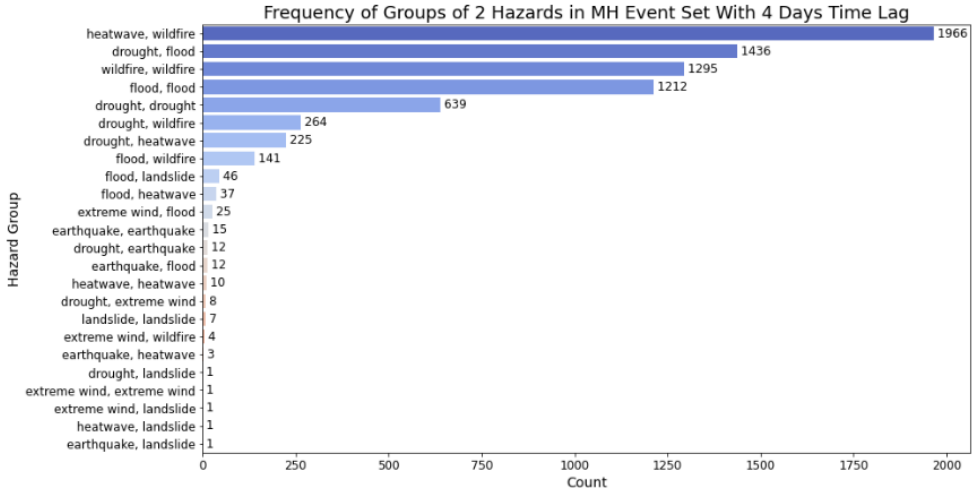

a) Groups of 2 hazards

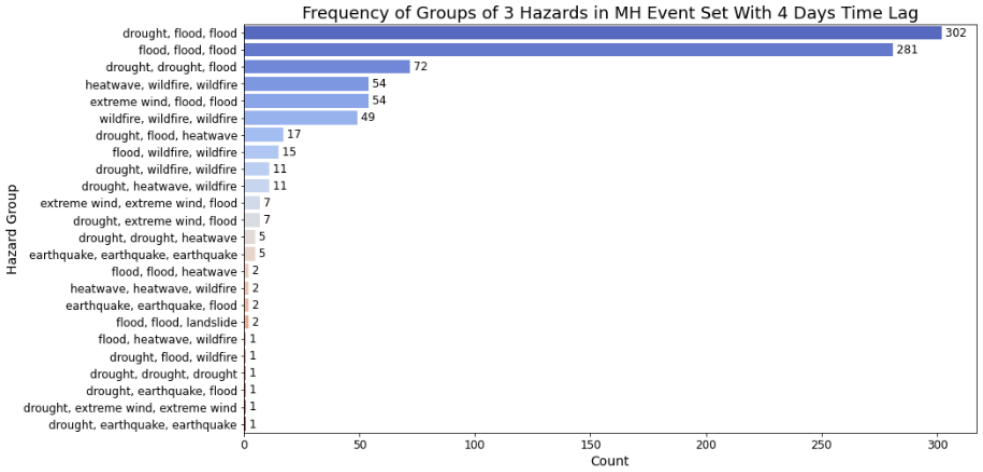

b) Groups of 3 hazards

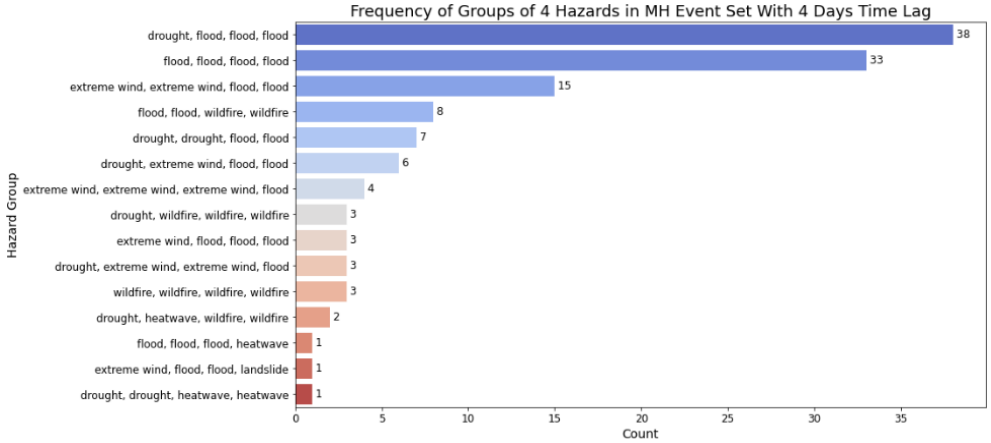

c) Groups of 4 hazards

Fig11*: a, b, & c the frequency of MH event sets with a 4-day time lag, groups of 2, 3, & 4 hazards respectively*

This project has received funding from the European Union's horizon Europe research and innovation program under grant agreement No. 101093854

5. Discussion and concluding remarks

In this task, we developed an event set for each of the seven climate hazards most relevant for the MIRACA project, and used these sets to create multi-hazard events by identifying spatial and temporal overlaps among single hazard events.

Results indicate that not considering time lags when grouping events can lead to missing important multi-hazard events. For example, earthquakes and landslides typically occur suddenly and do not last long, so there is a high probability of missing earthquake-induced landslides if time lags are not considered in our method.

The analysis shows that heatwaves and wildfires have a high occurrence in our multi-hazard event sets, while the combination of earthquakes and landslides is among the rarest (most likely explained due to the limited availability of landslide information). The indicator used for drought in this task is the low flow index, which relates to river areas. This may have excluded drought-affected areas from the multi-hazard event set if they did not overlap spatially with wildfires. Using different drought indicators that reflect conditions in other areas might result in different multi-hazard combinations.

It is important to note that this version of the MH-event sets, for both zero time lag and a 4-day time lag, is based on comparing entire single event sets without aligning their common time frames. For instance, the heatwave datasets span from 1987 to the present, while the wildfire datasets start from 2000. Additionally, the scarcity of data for some hazards and the abundance of data for others might lead to the dominance of specific types of hazards. For example, there are thousands of events in our datasets for wildfires and floods compared to hundreds for landslides or winter windstorms.

Data scarcity is a significant issue that can substantially affect the direction of a project. For example, hail events were also of interest for this task, but to the knowledge of the authors, there is no accessible data for hail events in Europe at the time of preparing this deliverable. Consequently, hail was excluded from this task. Similarly, landslides lacked a footprint or quantifiable intensity measures, requiring assumptions to be made. In addition, the absence of a standardized database necessitates time allocation for data cleaning and harmonization to enable comparisons and the creation of MH event datasets.

This project has received funding from the European Union's horizon Europe research and innovation program under grant agreement No. 101093854

The field of natural hazards is typically divided based on hazard type, and events are usually recorded individually, even when they occur alongside other hazards. This approach can lead to an incomplete understanding of the frequency and interconnections of natural hazards in a region. Therefore, a dataset that includes multiple hazards is crucial for studying natural hazards as a combination of all threats that may occur in a region. In this task, we reviewed all available events for different hazards in Europe and identified multi-hazard events. The assumptions made and the types of datasets used in this task influenced the results. Further studies on creating multi-hazard event datasets are necessary to enhance our understanding of multi-hazard events, their frequency, and the associated risks. Better understanding of multi-hazard events will shed light on ways to enhance the effectiveness of risk management and mitigation measures.

This project has received funding from the European Union's horizon Europe research and innovation program under grant agreement No. 101093854

References

Andela, N., Morton, D. C., Giglio, L., Paugam, R., Chen, Y., Hantson, S., ... & Randerson, J. T. (2019). *The Global Fire Atlas of individual fire size, duration, speed and direction*. Earth System Science Data, 11(2), 529-552.

Bachmair, S., Stahl, K., Collins, K., Hannaford, J., Acreman, M., Svoboda, M., ... & Overton, I. C. (2016). *Drought indicators revisited: the need for a wider consideration of environment and society*. Wiley Interdisciplinary Reviews: Water, 3(4), 516-536.

Claassen, J. N., Ward, P. J., Daniell, J., Koks, E. E., Tiggeloven, T., & de Ruiter, M. C. (2023). *A new method to compile global multi-hazard event sets*. Scientific Reports, 13(1), 13808.

Copernicus Climate Change Service, Climate Data Store, (2022): *Winter windstorm indicators for Europe from 1979 to 2021 derived from reanalysis*. Copernicus Climate Change Service (C3S) Climate Data Store (CDS). DOI: 10.24381/cds.9b4ea013 (Accessed on 05-03-2024)

Copernicus Emergency Management Service. (2018). Factsheet: Low Flow Index. https://drought.emergency.copernicus.eu/data/factsheets/factsheet_lowflowindex.pdf

De Ruiter, M. C., Couasnon, A., van den Homberg, M. J., Daniell, J. E., Gill, J. C., & Ward, P. J. (2020). *Why we can no longer ignore consecutive disasters*. Earth's future, 8(3), e2019EF001425.

Dottori, F., Mentaschi, L., Bianchi, A. et al. *Cost-effective adaptation strategies to rising river flood risk in Europe*. Nat. Clim. Chang. 13, 196–202 (2023). https://doi.org/10.1038/s41558-022-01540-0

European Commission, Joint Research Centre (JRC) (2021): E*DO Low Flow Index (LFI) (version 2.1.0)*. European Commission, Joint Research Centre (JRC) [Dataset] PID: http://data.europa.eu/89h/fd18fd1d-1af4-443a-b624-e19001b91f49

This project has received funding from the European Union's horizon Europe research and innovation program under grant agreement No. 101093854

Guo, A., Liu, Z., Li, S., & Li, H. (2017). *Seismic performance assessment of highway bridge networks considering post-disaster traffic demand of a transportation system in emergency conditions*. Structure and Infrastructure Engineering, 13(12), 1523–1537. https://doi.org/10.1080/15732479.2017.1299770

. Hersbach, H., Bell, B., Berrisford, P., Biavati, G., Horányi, A., Muñoz Sabater, J., Nicolas, J., Peubey, C., Radu, R., Rozum, I., Schepers, D., Simmons, A., Soci, C., Dee, D., Thépaut, J-N. (2023): *ERA5 hourly data on single levels from 1940 to present*. Copernicus Climate Change Service (C3S) Climate Data Store (CDS), DOI: 10.24381/cds.adbb2d47 (Accessed on 16-05-2024)

Joint Research Centre. (2024). *Current drought situation in Europe. European and Global Drought Observatories.* Retrieved July 6, 2024, from https://joint-research-centre.ec.europa.eu/european-and-global-drought-observatories/current-drought-situation-europe_en

Kirschbaum, D. B., Adler, R., Hong, Y., Hill, S., & Lerner-Lam, A. (2010). A *global landslide catalog for hazard applications: method, results, and limitations.* Natural Hazards, 52, 561-575.

Kirschbaum, D., Stanley, T., & Zhou, Y. (2015). *Spatial and temporal analysis of a global landslide catalog*. Geomorphology, 249, 4-15.

Koukis, G., et al. "*Landslide phenomena related to major fault tectonics: rift zone of Corinth Gulf, Greece." Bulletin of engineering geology and the* environment 68 (2009): 215-229.

McColl, S. T., & Cook, S. J. (2024). *A universal size classification system for landslides. Landslides,* 21(1), 111-120.

Li, S., Farrar, C., & Yang, Y. (2023). *Efficient regional seismic risk assessment via deep generative learning of surrogate models*. Earthquake Engineering & Structural Dynamics, 52(11), 3435-3454.

This project has received funding from the European Union's horizon Europe research and innovation program under grant agreement No. 101093854

Paprotny, D. (2024). *HANZE catalogue of modelled flood footprints in Europe, 1950-2020* (Version v1) [Data set]. Zenodo. https://doi.org/10.5281/zenodo.10640691

Paprotny, D. (2024). *HANZE catalogue of modelled flood footprints in Europe, 1950-2020 [Data set]*. Zenodo. https://doi.org/10.5281/zenodo.10640692

Paprotny, D., Rhein, B., Vousdoukas, M. I., Terefenko, P., Dottori, F., Treu, S., ... & Kreibich, H. (2024). *Merging modelled and reported flood impacts in Europe in a combined flood event catalogue,* 1950–2020. EGUsphere, 2024, 1-47. DOI: 10.5194/egusphere-2024-499, 2024

San-Miguel-Ayanz, J., Schulte, E., Schmuck, G., Camia, A., Strobl, P., Libertà, G., Giovando, C., Boca, R., Sedano, F., Kempeneers, P., McInerney, D., Withmore, C., Santos de Oliveira, S., Rodrigues, M., Durrant, T., Corti, P., Oehler, F., Vilar L., Amatulli, G. (2012) *Comprehensive monitoring of wildfires in europe: the European Forest Fire Information System (EFFIS), in John Tiefenbacher (Ed.), Approaches to Managing Disaster - Assessing Hazards, Emergencies and Disaster Impacts,* pp. 87-105, InTech, ISBN 978-953-51-0294-6.

St Cloud, E. H. R. M. (2022). TECHNICAL SPECIFICATIONS Volume 2: DIVISIONS 21-48.

Suarez-Gutierrez, L., Müller, W.A. & Marotzke, J. Extreme heat and drought typical of an end-of-century climate could occur over Europe soon and repeatedly. Commun Earth Environ 4, 415 (2023). https://doi.org/10.1038/s43247-023-01075-y

U.S. Geological Survey. (2024). Search Earthquake Catalog. Retrieved January 30, 2024, from https://earthquake.usgs.gov/earthquakes/search/

U.S. Geological Survey. (2024). ShakeMap. Retrieved January 30, 2024, from https://earthquake.usgs.gov/data/shakemap/

This project has received funding from the European Union's horizon Europe research and innovation program under grant agreement No. 101093854